

# Radiation-driven winds of hot luminous stars

## XV. Constraints on the mass–luminosity relation of central stars of planetary nebulae

A. W. A. Pauldrach<sup>1</sup>, T. L. Hoffmann<sup>1</sup>, and R. H. Méndez<sup>2</sup>

<sup>1</sup> Institut für Astronomie und Astrophysik der Universität München, Scheinerstraße 1, 81679 München, Germany

<sup>2</sup> Institute for Astronomy, University of Hawaii, 2680 Woodlawn Drive, Honolulu, HI 96822, U.S.A.

Received date / Accepted date

**Abstract.** We present a new model atmosphere analysis of nine central stars of planetary nebulae. This study is based on a new generation of realistic stellar model atmospheres for hot stars; state-of-the-art, hydrodynamically consistent, spherically symmetric model atmospheres that have been shown to correctly reproduce the observed UV spectra of massive Population I O-type stars. The information provided by the wind features (terminal velocity, mass loss rate) permits to derive the physical size of each central star, from which we can derive the stellar luminosity, mass, and distance, without having to assume a relation between stellar mass and luminosity taken from the theory of stellar structure and AGB and post-AGB evolution. The results of our analysis are quite surprising: we find severe departures from the generally accepted relation between post-AGB central star mass and luminosity.

**Key words.** stars: central stars of planetary nebulae – atmospheres – winds, outflows – evolution – fundamental parameters – early-type

### 1. Introduction

In recent years there has been substantial progress in the modelling of expanding atmospheres of hot stars. It is now possible to produce synthetic UV spectra of O stars that resemble the real, observed ones nearly perfectly. The state-of-the-art wind models deal with radiatively driven, homogeneous, stationary, extended, outflowing, spherically symmetric atmospheres. A complete model atmosphere calculation involves solving the hydrodynamics and the NLTE problem (rate equations for all important elements, radiative transfer, and energy equation). The solution of the total interdependent system of equations has thereby to be based on a non-restrictive treatment. This permits the calculation of the predicted or synthetic spectrum, which is then compared to the observed UV spectrum (cf. Pauldrach et al., 2001). The process is repeated adopting different stellar parameters until a satisfactory fit is obtained. In this kind of work it is not necessary to adopt an arbitrary velocity law for the wind; the solution is hydrodynamically consistent and gives us the velocity law as well as the mass-loss rate (cf. Pauldrach 2003, Pauldrach and Hoffmann 2003).

A very important consequence of these recent developments is that the fits to the UV spectral features provide information about all the basic stellar parameters: effective temper-

ature ( $T_{\text{eff}}$ ), radius ( $R$ ) – or equivalently, luminosity ( $L$ ) –, mass of the star ( $M$ ), terminal wind velocity ( $v_{\infty}$ ), and mass loss rate ( $\dot{M}$ ). Therefore we have a purely spectroscopic method to obtain separately  $L$  and  $M$ .

Using this new generation of realistic stellar model atmospheres, Pauldrach et al. (2001), Pauldrach (2003), and Pauldrach and Hoffmann (2003) present analyses of the massive O supergiants HD 30614 ( $\alpha$  Cam) and HD 66811 ( $\zeta$  Pup) which provide excellent matches to the observable UV-spectra, thus determining the basic stellar parameter sets of these objects. Further examples of this kind of work are given by Hoffmann and Pauldrach (2001), who confirm in their analysis of a subsample of galactic massive O stars the parameters derived by Puls et al. (1996) from an optical investigation.

Since this method produces reasonable results when applied to massive Population I stars, we now want to apply it to another kind of hot stars: the central stars of planetary nebulae (CSPNs in what follows). This permits, for the first time, to test the predictions from post-AGB evolutionary calculations. (The idea is described together with a first application by Pauldrach et al. 1988; preliminary results of the present investigation have been published by Pauldrach et al. 2001a.) The earlier work on CSPNs, based on plane-parallel non-LTE model atmospheres (e.g., Méndez et al. 1988a, 1988b) could not provide a completely independent test, in the following sense: since the plane-parallel model fits to H and He photospheric absorp-

tion lines can only produce information about surface temperature, He abundance and surface gravity ( $\log g$ ), we cannot derive stellar masses or luminosities, but only  $L/M$  ratios. This is exactly the same problem we face when dealing with low-gravity early-type “supergiant” stars at high Galactic latitudes: are they luminous and massive, or are they evolving away from the AGB? We need some independent evidence to settle the issue – for example, the distance to the star. Unfortunately, we lack reliable distances to almost all CSPNs.

What could be done was to plot the positions of CSPNs in the  $\log g$ – $\log T_{\text{eff}}$  diagram, and compare them with plots of post-AGB tracks, translated from the  $\log L$ – $\log T_{\text{eff}}$  diagram. After doing this translation it is possible to read the stellar mass in the  $\log g$ – $\log T_{\text{eff}}$  diagram. From this, we can derive  $L$  and, if we know the visual dereddened apparent magnitude, a so-called “spectroscopic distance”. All this work, however, is based on *assuming* that the evolutionary models give us the correct relation between stellar mass and luminosity. It is not a real test of the evolutionary models, but only a consistency check.

The new models allow us to overcome this limitation and produce for the first time information on  $L$  and  $M$  which is completely independent from the theory of stellar structure and evolution. In this paper we present the initial outcome of the project. We have made a careful selection of CSPNs for which we have adequate spectrograms covering both the visible and UV spectrum. In Sections 2 and 3 we describe the available spectrograms. In Section 4 we present the necessary information about the new wind models and we outline the fitting procedure. Section 5 introduces the relation between wind momentum loss rate and stellar luminosity, predicted by the theory of radiatively driven winds, and briefly describes earlier efforts to verify if the CSPNs follow this relation. Then in Sections 6 and 7 we present the UV spectral fits using the new wind models, explaining what discrepancies there are with respect to the earlier modelling and producing a table with the stellar parameters determined. Section 8 gives the interpretation of the CSPN winds and a discussion of the results concerning stellar luminosities and masses. In Section 9 we estimate the spectroscopic distances and compare them with other distance determinations, with inconclusive results. Section 10 deals with other estimates of pre-white dwarf masses. In Section 11 we summarize the conclusions.

## 2. The UV spectrograms

The sample of CSPNs we have analyzed is defined by the availability of adequate high-resolution UV spectra, covering the spectral region between 1000 and 2000 Å.

With the exception of that of He 2-108, all UV spectra of our sample were obtained from the INES Archive Data Server on the Web at <http://ines.laeff.esa.es/>, providing access to IUE Final Archive data. Apart from rectification “by eye” (aided by our experience with UV spectra from massive O stars), no further processing was done on the spectra.

The spectrum of He 2-108 is an HST/FOS spectrum (Proposal ID 5339, PI RHM) rectified by Haser (1995). Here, interstellar Lyman- $\alpha$  absorption has been taken into account

in the rectification process, leading to an empty band around 1216 Å with noisy edges.

## 3. The optical spectrograms

Most of the optical spectrograms were obtained by one of us (RHM) during two observing runs at the European Southern Observatory (ESO), Cerro La Silla, on 21–24 March and 13–17 June 1994 (the first one by remote control from ESO Garching), using the 3.5 m New Technology Telescope (NTT) and EMMI spectrograph in dichroic mode. In this mode of operation a dichroic beam-splitter was inserted, allowing to obtain blue and red spectrograms simultaneously.

A long slit of 1 arc sec width was used in the focal plane. The slit was oriented either N-S or E-W.

The dispersing element in the blue arm was grating number 3, with 1200 lines/mm, and the camera was  $f/4$ , giving a pixel size of 0.37 arc sec and a dispersion of 0.42 Å/pixel. The detector was a Tektronix CCD, 1124 × 1024 pixels, with pixel size of 24  $\mu\text{m}$ . In order to decrease the readout time only the central 200 pixels along the slit were read. Therefore the resulting spectrograms covered 74 arc secs along the slit, and 450 Å in wavelength, with central wavelengths of 4500 Å and 4535 Å in March and June 1994, respectively.

The dispersing element in the red arm was grating number 6, with 1200 lines/mm, and the camera was  $f/5.2$ , giving a pixel size of 0.27 arc sec and a dispersion of 0.31 Å/pixel. The detector was a Tektronix CCD, 2086 × 2048 pixels, with pixel size of 24  $\mu\text{m}$ . In order to decrease the readout time only the central 400 pixels along the slit were read. Therefore the resulting spectrograms covered 108 arc secs along the slit, and 650 Å in wavelength, with central wavelengths of 6560 Å and 6505 Å in March and June 1994, respectively.

The exposure times were short in the red arm, to avoid saturation of the strongest nebular emission lines.

The usual calibration frames (bias, dome flats, He-Ar comparison spectrum for wavelength calibration) were obtained for the observations in both arms. The CCD reductions were made using standard tasks provided in IRAF<sup>1</sup>. After bias-level subtraction and flatfielding, whenever possible the spectrograms were registered and combined, to eliminate cosmic ray events and improve the signal-to-noise ratio. The image combination was made with the IRAF task *imcombine*, using the *average* option and *ccdclip* rejection (pixel rejection based on CCD noise parameters).

## 4. The modelling procedure

The UV spectrum between 1000 and 2000 Å carries a lot of information: P-Cygni-type profiles of resonance lines of several ions of C, N, O, Si, S, P, as well as hundreds of strongly wind-contaminated lines of Fe IV, Fe V, Fe VI, Cr V, Ni IV, Ar V, Ar VI. But the information about the stellar parameters can be

<sup>1</sup> IRAF is distributed by the National Optical Astronomical Observatories, operated by the Association of Universities for Research in Astronomy, Inc., under contract to the National Science Foundation of the U.S.A.

extracted only after careful analysis. A very important recent improvement of our method concerns the development of a substantially consistent treatment of the blocking and blanketing influence of all metal lines in the entire sub- and supersonically expanding atmosphere. All the results we will present are based on this new generation of models.

The analysis method is based on modelling a homogeneous, stationary, extended, outflowing, spherically symmetric radiation-driven atmosphere. A detailed description is given by Pauldrach et al. (2001), Pauldrach (2003), and Pauldrach and Hoffmann (2003).

The procedure is as follows. A preliminary inspection of the visual and/or UV spectrum of the star to be analyzed gives an estimate of  $T_{\text{eff}}$ . From the UV spectrum, the terminal wind velocity  $v_{\infty}$  can be measured directly. Now initial values for the stellar radius  $R$  (defined at a Rosseland optical depth of  $2/3$ ) and for the stellar mass  $M$  are assumed.

With the current values of  $R$ ,  $T_{\text{eff}}$ ,  $M$ , and assuming a set of abundances, we can solve the model atmosphere and calculate the velocity field, the mass loss rate  $\dot{M}$ , and the synthetic spectrum. If the calculated terminal wind velocity  $v_{\infty}$  of the model differs from the observed one, we modify  $M$  until agreement is reached (since  $v_{\infty}$  scales with  $(M/R)^{1/2}$  according to the theory of radiation-driven winds). Now the predicted spectrum is compared to the observed one. If the fit is not satisfactory, we need to modify  $\dot{M}$  via a change of  $R$  (since  $\log \dot{M} \sim \log L$ , according to radiation-driven wind theory). The change in  $R$  forces us to change the mass, too, in order to keep  $v_{\infty}$  consistent with the observed value. The new model is calculated and the process is repeated until we obtain a good fit to all features in the observed spectrum. (Additionally,  $T_{\text{eff}}$  might need to be corrected slightly during this iteration, if the initial guess was not satisfactory.)

With this procedure our current models produce satisfactory results for massive Population I stars. What happens if we apply the same procedure to CSPNs?

## 5. The wind properties of hot stars

As a first point of our investigation we examine the dynamical parameters  $v_{\infty}$  and  $\dot{M}$  of radiation-driven CSPN winds.

The significance of this parameters is obvious, since it is the consistent hydrodynamics which provides the link between the stellar parameters ( $T_{\text{eff}}$ ,  $M$ ,  $R$ ) and the appearance of the UV spectra, because the latter are determined by the interplay of the NLTE model and the hydrodynamics. The link is the line force which controls the hydrodynamics, and which is controlled by the occupation numbers, and the radiative transfer of the NLTE model. The hydrodynamics in turn affects the NLTE model and thus the spectra via the density and velocity structure.

### 5.1. The relation between wind-momentum loss rate and luminosity

A tool for illustrating the behavior of the dynamical parameters is offered by the so called *wind-momentum–luminosity relation*.

The significance of this relation is based on the fact that, due to the driving mechanism of hot stars, the mechanical

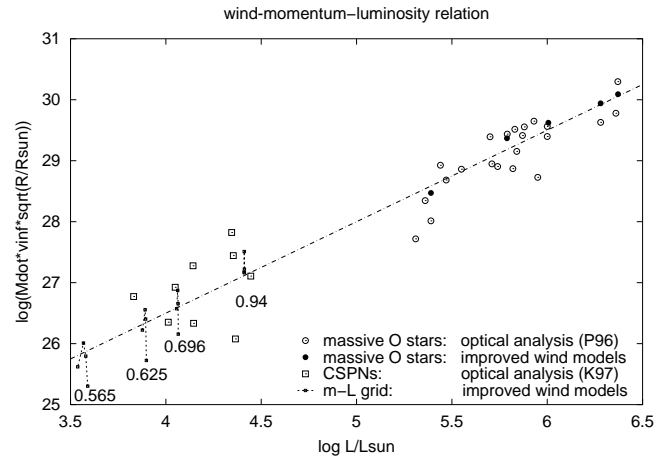


**Fig. 1.** The wind-momentum–luminosity relation for massive O stars and CSPNs. P96 designates the analysis based on  $H\alpha$  profiles by Puls et al. 1996, K97 that of CSPNs by Kudritzki et al. 1997. Also plotted are the calculated wind momenta for a sample of massive O stars and for a grid of stars following post-AGB evolutionary tracks (masses given in  $M_{\odot}$ ).

momentum of the wind flow ( $v_{\infty}\dot{M}$ ) is mostly a function of photon momentum ( $L/c$ ) and is therefore related to the luminosity. Thus, the radiatively driven wind theory predicts, for fixed abundances, a simple relation between the quantity  $\dot{M}v_{\infty}$ , which has the dimensions of a momentum loss rate, and the stellar luminosity:

$$\dot{M}v_{\infty} \sim R^{-1/2}L^{1/\alpha}$$

where  $\alpha$ , related to the power law exponent of the line strength distribution function, is  $\simeq 2/3$  (slightly dependent on temperature and metallicity; see, for example, Puls et al. 1996). As the expression  $v_{\infty}\dot{M}R^{1/2}$  is an almost directly observable quantity (see below), it is practical to plot the log of  $\dot{M}v_{\infty}R^{1/2}$  as a function of  $\log L$ . In this kind of plot the theory predicts, in first approximation, a linear relation, which is indeed followed by all kinds of massive hot stars, as shown in Figure 1.

An initial attempt to verify if CSPNs follow the wind-momentum–luminosity relation was partly successful (see Figure 3 in Kudritzki et al. 1997 and also our Figure 1). In that paper, terminal wind velocities  $v_{\infty}$  were taken from observed UV spectra and  $Q$ -values (a quantity relating mass loss rate and stellar radius,  $Q \sim \dot{M}(Rv_{\infty})^{-3/2}$ ) were derived from observed  $H\alpha$  profiles<sup>2</sup> using the optical spectra described in section 3. Stellar masses were derived from  $T_{\text{eff}}$  and  $\log g$ , using post-AGB tracks plotted in the  $\log g$ – $\log T_{\text{eff}}$  diagram. The stellar radii (and thus, mass loss rates) and luminosities were then obtained from the masses and the post-AGB mass–luminosity relation. The CSPNs were found to be at the expected position along the wind-momentum–luminosity relation, indicating a qualitatively successful prediction by the theory of ra-

<sup>2</sup> We refer to this as “optical analysis”, since although  $v_{\infty}$  was taken from UV spectra, this is a quantity that can be derived easily and does not require much analysis. The real analysis determining  $Q$  and  $\log g$  using model atmospheres was performed using optical spectra.

diatively driven winds. However, the situation was not satisfactory because there appeared to be a large dispersion in wind strengths at a given luminosity (strong-winded and weak-winded CSPNs) and some of the CSPN masses and luminosities were very high ( $M > 0.8 M_{\odot}$ ), in contradiction with theoretical post-AGB evolutionary speeds.

Thus, at that point we had a qualitatively positive result, namely that in principle the CSPN winds appear to obey the same physics as the massive O star winds; but we also had some unsolved problems.

This situation has been recently discussed by Tinkler and Lamers (2002), who try to improve the central star parameters by imposing consistency between the evolutionary age of the central star and the dynamical age of its PN. As result of scaling the distances and stellar parameters according to their method they obtain a scatter diagram with no clear dependence of wind momentum on luminosity. So in this way we find a conflict between the predictions of post-AGB evolution theory and the theory of radiatively driven stellar winds! Are the post-AGB evolutionary tracks not complete? Or is the behavior of the photon-momentum transfer different in the atmospheres of O-type CSPNs and massive O-stars?

We now want to rediscuss this situation using our improved model atmospheres.

As a preparatory step we have used our models to calculate the terminal velocities and mass loss rates for a grid of stars following the current theoretical post-AGB evolutionary tracks with surface temperatures from 30000 to 90000 K (see, for instance, Blöcker 1995); the resulting wind momenta are also plotted in Figure 1 (labelled “m–L grid”). The numerical models do nicely follow, as expected, the theoretical wind momentum–luminosity relation, showing less spread than the “observed” values derived by Kudritzki et al. (1997). The positions of the Kudritzki et al. values in the diagram, compared to those of our models, again indicate rather large masses between 0.6 and 0.95  $M_{\odot}$ , with a clear absence of CSPNs with masses below 0.6  $M_{\odot}$ .

As explained before, to find so many very massive CSPNs is rather unexpected from the standpoint of current evolutionary theory, in view of their very high predicted evolutionary speeds.

### 5.2. The relations of the individual dynamical parameters $v_{\infty}$ and $\dot{M}$

To try to better understand the discrepancy found from the investigation of the wind momenta, we must compare the relations of the individual dynamical quantities involved ( $v_{\infty}$  and  $\dot{M}$ ), since these relations are not just a function of the stellar luminosity, as is the case for the “wind-momentum–luminosity relation”, they are also sensitively dependent on the stellar mass.

By doing so we find indeed that something must be seriously wrong. Figure 2 (upper panel) shows our predicted terminal velocities and the observed values. Figure 2 (lower panel) shows our predicted mass loss rates and those derived by Kudritzki et al. (1997) for their sample. Here a fundamental

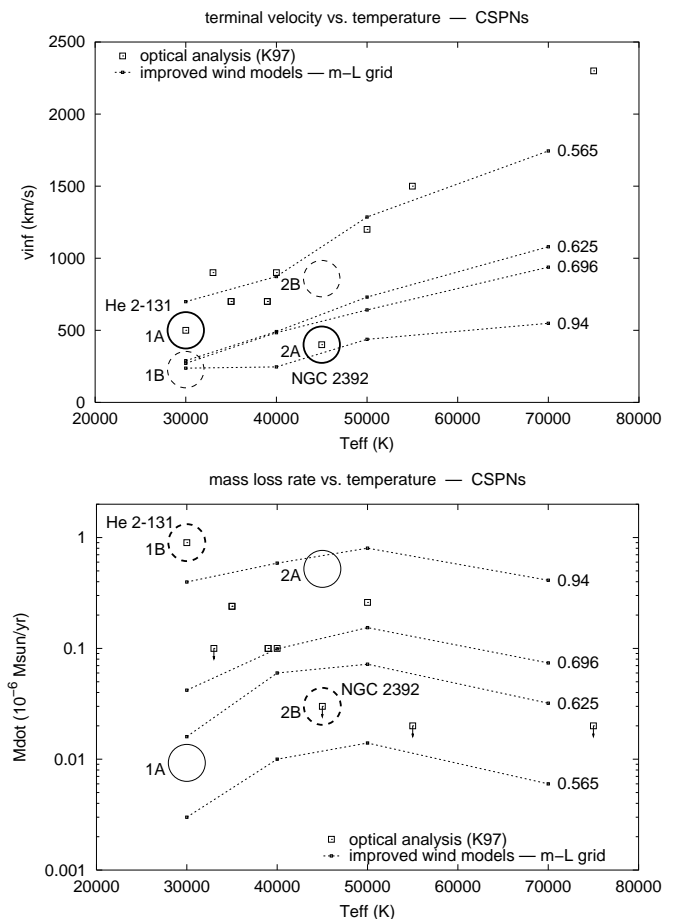


**Fig. 2.** Terminal velocities (upper panel) and mass-loss rates (lower panel) calculated for a grid of stars following post-AGB evolutionary tracks (dashed lines, masses in  $M_{\odot}$  labelled on the right) compared to observed values derived by Kudritzki et al. (1997) (squares). Note that the observed terminal velocities and mass-loss rates indicate different masses for the same objects (circles) – for a discussion see text.

discrepancy immediately becomes obvious: whereas the positions of the observations in the diagram showing the terminal velocities cluster at rather small CSPN masses (between 0.5 and 0.6  $M_{\odot}$ ), their mass loss rates point to a majority of masses above 0.7  $M_{\odot}$ .

A detailed look at the positions of individual CSPNs in the plots reveals even more alarming discrepancies. Take, for example, He 2-131. Its terminal velocity would indicate a mass of about 0.6  $M_{\odot}$  (circle 1A in Figure 2 upper panel). But this mass is completely irreconcilable with its mass loss rate: it is found not at the position labelled 1A in Figure 2 (lower panel), but at 1B, with  $\dot{M}$  a factor of hundred higher, suggesting a mass of above 0.94  $M_{\odot}$ ! The reverse is true for NGC 2392. Its terminal velocity points to a mass of about 0.9  $M_{\odot}$  (circle 2A in Figure 2 upper panel), but its observed mass loss rate is much too small for this mass (circle 2B in Figure 2 lower panel), indicating a mass of approximately 0.6  $M_{\odot}$ .

If instead of the terminal velocities we take the mass loss rate determinations of Kudritzki et al. (1997) as basis for the

discussion, then our calculations place these two stars at the positions labelled 1B and 2B in Figure 2 (upper panel), with terminal velocities differing by factors of 2 to 3. But this is clearly ruled out by the observations;  $v_\infty$  is a directly measurable quantity!

Therefore, no matter how we look at these plots, we conclude that the analysis of Kudritzki et al. (1997) revealed mass loss rates which cannot be reconciled with the currently accepted post-AGB evolutionary tracks which the radiatively driven wind models shown have been based on.

So far we have used from the UV spectra of the CSPNs only one bit of information: the observed terminal velocity  $v_\infty$ . Now we will try to clarify the situation by fitting the full UV spectra with the new atmospheric models. In this way the wind theory will provide us with stellar parameters derived independently of the post-AGB evolution theory, and in case we are successful by fitting the spectra consistently with the dynamical parameters we might have the chance to decide whether the reason for this discrepancy lies with the evolutionary tracks on the one hand or the analysis by Kudritzki et al. (1997) on the other.

## 6. Consistent UV analysis of the CSPNs He 2-131 and NGC 2392

We will start with a detailed description of the two puzzling cases we have been squarely faced with above.

Figure 3 (top left) shows the synthetic UV spectrum of the model corresponding to position 1A in Figure 2. It is clearly incompatible with the observed spectrum<sup>3</sup> of He 2-131 (middle), since its mass loss rate and due to that its luminosity is obviously too small, as evidenced by the presence of mostly purely photospheric lines, hardly affected by the unincisive thin wind. The theory of radiation-driven winds offers a solution: this CSPN must have a much larger luminosity, because  $L$  is the major factor determining the mass loss rate. We have calculated a series of models with increasing luminosity – and therefore increasing mass loss rate – (at the same time adjusting the mass to keep the terminal velocity at its observed value) to verify if one of these models could reproduce the numerous strongly wind-contaminated iron lines observed especially between 1500 and 1700 Å. Indeed, a more luminous model, able to sustain the high mass loss rate of model 1B in Figure 2, produces a convincing fit – see Figure 3, bottom left. The parameters of this model are given in Table 1.

The situation is reversed with NGC 2392. The synthetic spectrum of model 2A in Figure 2 is incompatible with the observed UV spectrum (Figure 3, right top and middle, respectively), since it produces many strongly wind-contaminated lines, which are not observed; the star produces almost exclusively photospheric lines! Again the problem can be attributed to the luminosity, which is too high in this case. Decreasing the

<sup>3</sup> Note that here and in the following, the observed spectra are contaminated by interstellar Lyman- $\alpha$  absorption. We have not attempted to include this in our models, since the affected region has no bearing on our conclusions. Neither are other interstellar lines included in the modelling procedure.

luminosity and thus the mass loss rate yields a model which is quite well in agreement with the observed spectrum (Figure 3, bottom right). The stellar parameters of this model are also given in Table 1.

In summary, the new model atmospheres produce a good fit to all the observable features in the UV spectrum. We remark at this point that our error in the stellar mass is very small ( $\leq 0.1 M_\odot$ ) due to the sensitive dependence on the predicted  $v_\infty$  and the small error received from determining this value from the observed spectrum ( $\leq 10\%$ ). Furthermore, we note that our predicted values of  $v_\infty$  are in agreement within 10% with the observed values in the case of massive O stars (cf. Hoffmann and Pauldrach 2001). Thus, a possible internal error leaves no margin for a larger uncertainty in the deduced masses.

What can we conclude from the derived stellar parameters? Let us consider first the weak-winded CSPN, NGC 2392. We determine a  $T_{\text{eff}}$  of 40000 K from the ionization equilibrium of Fe ions in the stellar UV spectrum, similar to the value obtained from the ionization equilibrium of He I and He II (absorption lines in the optical stellar spectrum).<sup>4</sup> The very low terminal wind velocity of  $400 \text{ km s}^{-1}$ , together with the low luminosity (needed to adjust the predicted mass loss rate so that the predicted and observed spectra are in good agreement) lead us to adopt a small radius. Using this radius ( $1.5 R_\odot$ ) and  $v_\infty$  we get a stellar mass of only  $0.41 M_\odot$ , a value much smaller than obtained if we assume the classical post-AGB mass–luminosity relation – a high mass of  $0.9 M_\odot$  was the result found by Kudritzki et al. (1997).

Note that the radius  $1.5 R_\odot$  and mass  $0.41 M_\odot$  of this CSPN correspond to  $\log g = 3.7$ , in good agreement with the  $\log g$  derived earlier from the NLTE plane-parallel analysis of the optical stellar spectrum.

In the case of the central star of He 2-131 the terminal velocity of  $500 \text{ km s}^{-1}$  (and  $T_{\text{eff}} = 33000 \text{ K}$ ) would appear to suggest, according to the classical post-AGB mass–luminosity relation (cf. Figure 2 upper panel), a stellar mass of about  $0.6 M_\odot$ . However, the wind features observed in the UV spectrum forced us to increase the stellar  $R$  and thus  $L$ , which in turn increased  $\dot{M}$  until a good fit was obtained. From the corresponding large radius –  $5.5 R_\odot$  – and  $v_\infty$  we derive a stellar mass of  $1.39 M_\odot$ , a value very close to the Chandrasekhar mass limit for white dwarfs! Thus, in this case the resulting mass is even more extreme than the value of  $0.9 M_\odot$  obtained by Kudritzki et al. (1997).

## 7. Consistent UV analysis of 7 additional CSPNs

In a similar fashion as for the two objects described in detail in the previous section, we have computed hydrodynamical

<sup>4</sup> We do not want to hide the fact that this central star has an anomalously high He II Zanstra temperature of about 70000 K and an even higher energy-balance temperature (Méndez et al. 1992), but we have carefully verified that both the visual and especially the UV stellar features are decidedly incompatible with such high temperatures. This discrepancy is at present unresolved. Apparently an additional source of He-ionizing photons is needed in this case. For the moment we ignore this, and perform the analysis using the information about  $T_{\text{eff}}$  derived from the stellar spectrum.

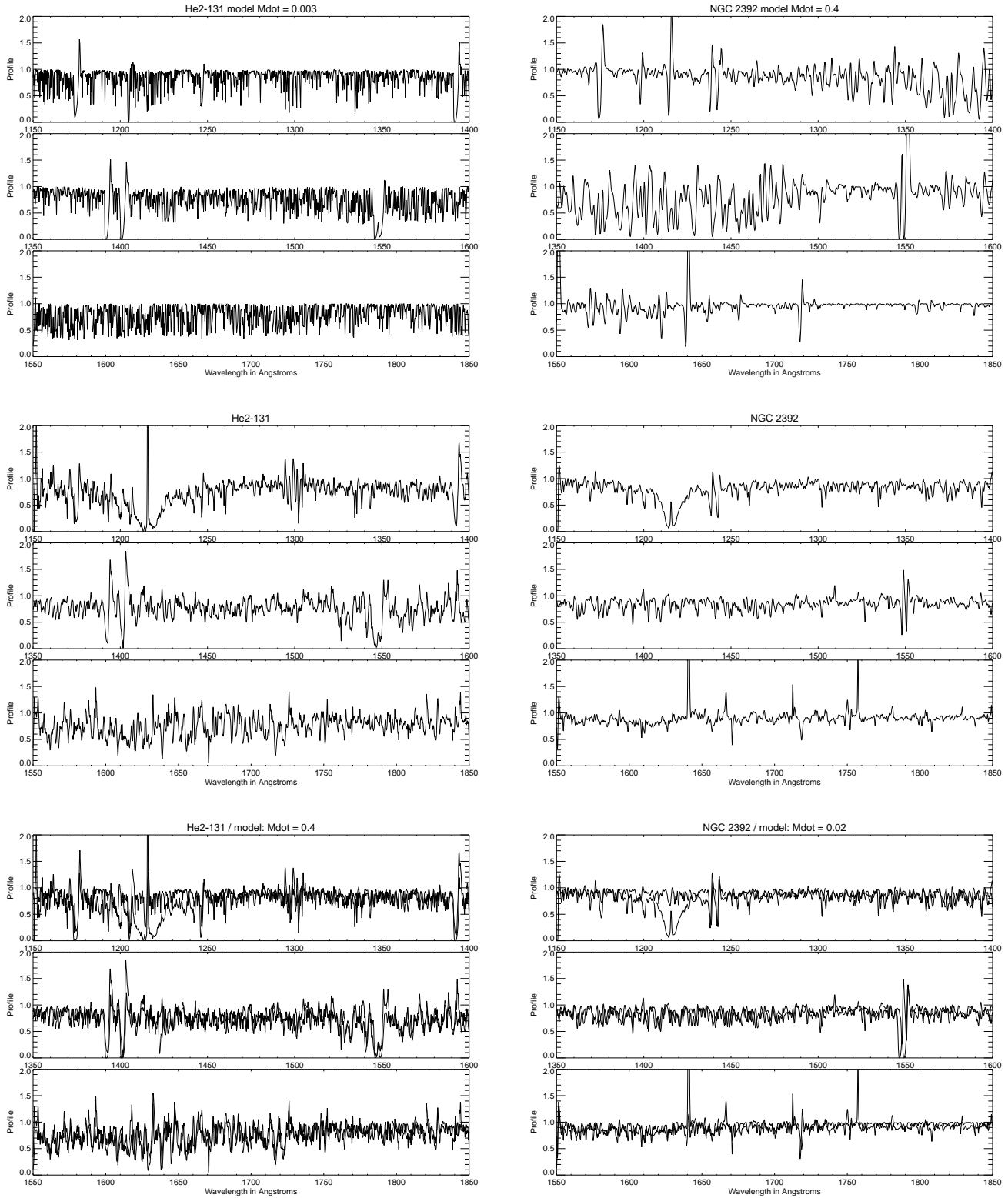


**Fig. 3.** (Left) Top: Synthetic spectrum of model 1A for He 2-131 (see text). This is incompatible with the observed IUE spectrum (middle). A model with a significantly enhanced luminosity which gives a higher mass loss rate, reproduces the distinctive features in the UV spectrum much better (bottom, overplotted with the observed spectrum to better show the similarity). (Right) Top: Synthetic spectrum of model 2A for NGC 2392. Again, this is incompatible with the observed IUE spectrum (middle). In this case, however, the luminosity ( $L$ ) and thus the mass loss rate is much too high, whereas a model with a lower luminosity reproduces the observed spectrum (bottom).

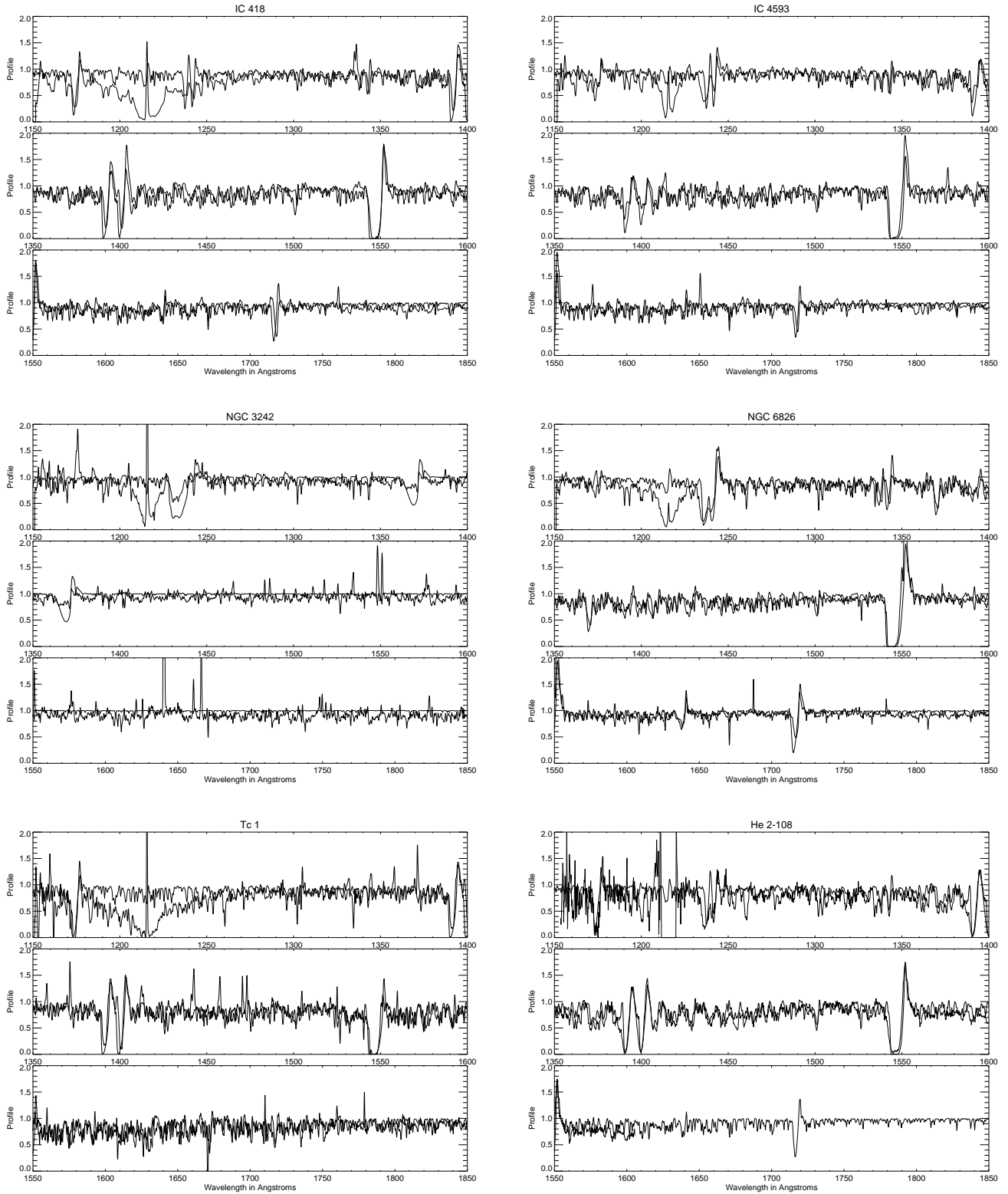


**Fig. 4.** Synthetic UV spectra from consistent atmospheric models for the other 6 CSPNs of our sample, compared to the observed UV spectra: IC 418 and IC 4593 (*top*), NGC 3242 and NGC 6826 (*middle*), and Tc 1 and He 2-108 (*bottom*).

models that reproduce the observed UV spectra of the 7 other CSPNs of our sample. The spectra are plotted in Figure 4, the resulting parameters are listed in Table 1.

We would like to remark on two points in this context. The first is that the observed spectrum of IC 4637 (not shown) is very noisy. Our parameters given for this particular star are therefore not of the same quality as those of the other objects, and should thus be seen more as a hydrodynamic consistency check to the values derived by Kudritzki et al. (1997), than as resulting from a detailed spectral fit.

The second is that the UV spectra of IC 418 and He 2-108 are very similar, and we therefore derive similar parameters for these two stars, as the same model obviously fits both spectra equally well.

Concerning the elemental composition, we have adopted the Helium abundances from Kudritzki et al. (1997). For the other elements, we have assumed a solar abundance pattern, justified by the good fit to the observed UV spectra. A minor discrepancy is seen in NGC 2392, which the optical spectrum would indicate to be N-rich and C-deficient, a result also reflected in the UV spectrum (for example, both the observed C III and C IV lines are weaker than those of the model). However, the influence of this on the hydrodynamics is small, since C and N are not major contributors to the line force (Pauldrach 1987) and the sum of C, N, and O would remain constant if these abundances were the result of the CNO-process.

## 8. Interpretation of CSPN winds

Table 1 shows the result of applying the method and UV analysis to the nine CSPNs of our sample.

First of all, these results are, in a broad sense, encouraging. We have not found any object with decidedly impossible masses and luminosities (for example, we could have derived masses and luminosities typical of massive Pop. I stars: certainly that would have been quite embarrassing, but it did not happen). However, a closer look shows that we are in a very unexpected situation.

Figure 5 shows the relation between stellar mass and luminosity obtained from our model atmosphere analyses, in comparison with the mass–luminosity relation of the evolutionary tracks, represented by the values from Kudritzki et al. (1997). From the viewpoint of current stellar evolutionary calculations this plot is somewhat unsettling: there is a very large spread in masses, between 0.4 and 1.4  $M_{\odot}$ , and the derived masses and luminosities do not agree with the classical post-AGB mass–luminosity relation. Most CSPNs are underluminous for their mass (or too massive for their luminosities).

In Figure 6 we show again the wind-momentum–luminosity relation for both massive hot stars and CSPNs, but this time based on the parameters derived in our analysis. Our new parameters give wind momenta of the right order of magnitude and within the expected luminosity range (there may be still too many CSPNs at  $\log L/L_{\odot} > 4$ , but not so many as in Kudritzki et al. 1997). The CSPNs are found along the extrapolation of the wind-momentum–luminosity relation defined by the massive hot stars, and the CSPNs show a smaller dispersion, i.e., a tighter correlation of wind-momentum with luminosity, than

was the case in Kudritzki et al. (1997). None of these facts is surprising, because our derived parameters are now based on the wind theory; of course the theory, consistently applied, will not produce any departure from its own predictions! However, the really significant fact is that we could produce a very convincing fit simultaneously to a multitude of diagnostic features in the CSPN UV spectra. There was no guarantee a priori that such a good overall fit was possible, and this is the main reason why we think that it is not easy to simply argue “the wind models must be wrong”. Instead, it is very likely that the theory and the models as an approach to it are correct in case the experiment in the form of a comparison of observed and synthetic UV-spectra was successful.

More importantly, the results obtained for NGC 2392 and NGC 3242 rule out the possibility that our method simply systematically overestimates the stellar masses: for these two stars we derive masses that lie below those deduced by Kudritzki et al. (1997). In the extreme case of NGC 2392, any systematic overestimate of the mass would require this star to have a mass even below 0.4  $M_{\odot}$ . If there is any physical effect at work whose neglect results in a systematic error in the analysis, it would need to be such that it can lead to an over- as well as underestimate of the masses, despite reproducing nearly perfectly the observed UV spectra. Our current knowledge of stellar winds does not provide us with any mechanism able to do this.

If we drop the *assumption* made by Kudritzki et al. that the stars obey the theoretical post-AGB mass–luminosity relation, and instead scale their mass loss rates to our radii<sup>5</sup> – keeping  $Q$ , the real observational quantity, fixed – then their wind momenta match ours to within about a factor of two. Furthermore, their sample with the radii thus scaled now also shows a much tighter correlation of the wind momentum to luminosity than before (see Figure 6). This indicates that **two independent procedures** to obtain the mass loss rates (one based on optical, the other based on UV wind-sensitive line profiles) **have given consistent results**. In other words, the problem cannot be attributed exclusively to the observational data used by Kudritzki et al. (1997) to estimate the mass loss rates.

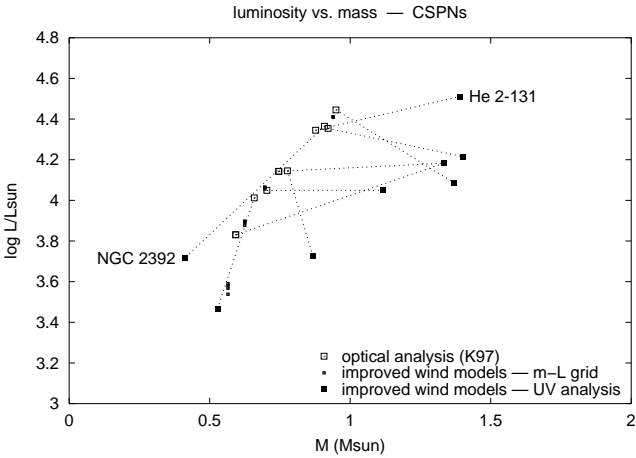
If we believe both, the current evolutionary theory and the luminosities and masses we have determined from the atmospheric models, then most of our CSPNs have not followed a classical post-AGB evolution. We find many stars near the Chandrasekhar limit for white dwarfs. They do not obey the core-mass–luminosity relation (being underluminous for their mass) and this indicates that their internal structure must be different. The special case of NGC 2392 is also remarkable: with such a small mass it cannot be a post-AGB star, and we would be forced to consider alternative evolutionary histories, involving probably a binary system merged immediately after the first visit to the red giant branch. A few similar cases of low-mass CSPNs have been noted in the past: EGB 5 and PHL 932, see Méndez et al. (1988a, 1988b). What makes NGC 2392 a more troublesome case is the additional fact that kinematically it is a rather young PN, while numerical simulations of binary merg-

<sup>5</sup> Additionally allowing for their different effective temperatures by requiring that the observed visual flux ( $\sim R^2 T_{\text{eff}}$ ) stay constant.



**Table 1.** Parameters of nine CSPNs derived from our analysis of the UV spectra using our model atmospheres, compared to the values found by Kudritzki et al. 1997.

Object	$T_{\text{eff}}$ (K)	$R$ ( $R_{\odot}$ )	$\log \frac{L}{L_{\odot}}$	$M$ ( $M_{\odot}$ )	$\log g$ (cgs)	$\dot{M}$ ( $10^{-6} M_{\odot}/\text{yr}$ )	$v_{\infty}$ (km/s)
our models							
NGC 2392	40000	1.5	3.7	0.41	3.70	0.018	420
NGC 3242	75000	0.3	3.5	0.53	5.15	0.004	2400
( IC 4637	55000	0.8	3.7	0.87	4.57	0.019	1500 )
IC 4593	40000	2.2	4.0	1.11	3.80	0.062	850
He 2-108	39000	2.7	4.2	1.33	3.70	0.072	800
IC 418	39000	2.7	4.2	1.33	3.70	0.072	800
Tc 1	35000	3.0	4.1	1.37	3.62	0.021	900
He 2-131	33000	5.5	4.5	1.39	3.10	0.35	450
NGC 6826	44000	2.2	4.2	1.40	3.90	0.18	1200
Kudritzki et al. 1997							
NGC 2392	45000	2.5	4.4	0.91	3.6	$\leq 0.03$	400
NGC 3242	75000	0.6	4.0	0.66	4.7	$\leq 0.02$	2300
IC 4637	55000	1.3	4.1	0.78	4.1	$\leq 0.02$	1500
IC 4593	40000	2.2	4.0	0.70	3.6	0.1	900
He 2-108	35000	3.2	4.1	0.75	3.3	0.24	700
IC 418	37000	3.5	4.3	0.89	3.3	0.26	700
Tc 1	33000	5.1	4.4	0.95	3.0	$\leq 0.1$	900
He 2-131	30000	5.5	4.3	0.88	2.9	0.9	500
NGC 6826	50000	2.0	4.4	0.92	3.8	0.26	1200

**Fig. 5.** Luminosity vs. mass for the evolutionary tracks (open squares) compared to the observed quantities determined with our method (filled squares). Although the luminosities deduced from the UV spectra lie in the expected range, a much larger spread in the masses (from 0.4 to  $1.4 M_{\odot}$ ) is obtained. The relation between CSPN mass and luminosity deviates severely from that taken from the theory of post-AGB evolution. Of course the latter is followed by the open squares and dots, because in that case it had been assumed from the start.

ing lead to expect no visible nebulae around them, or at most very old ones, like EGB 5 and PHL 932.

If we reject such drastic departures from the classical post-AGB evolutionary picture, still assuming the evolutionary calculations to be correct, then we would need to conclude that

our models, while adequate for massive O supergiants, are a failure for stars of similar surface temperature and gravity in another evolutionary status, and produce good fits to the CSPN UV spectra only by a surprising and misleading coincidence. Considering the successes of radiatively-driven wind theory, however, we regard this conclusion as highly improbable. We must therefore contemplate the possibility that our current knowledge of stellar evolution might be incomplete.

## 9. Spectroscopic distances and white dwarf masses

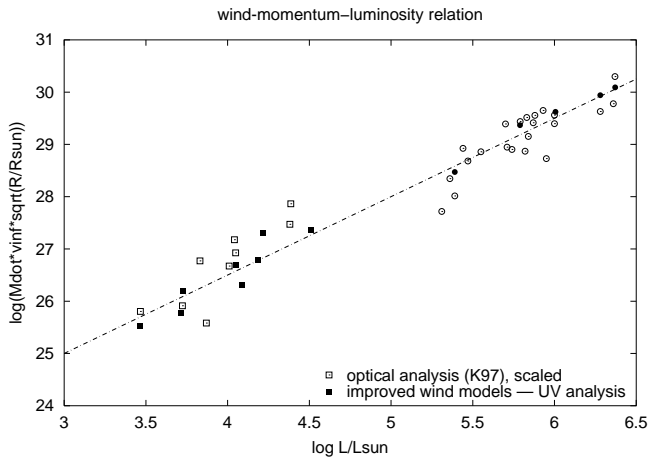
Facing this surprising situation, we ask if there is any way of further verifying the CSPN masses and luminosities we determined. One possible way is to calculate the spectroscopic distances and verify if they agree with the rest of the available evidence. Another way, since we expect CSPNs to become white dwarfs, is to look into what is currently known about the white dwarf mass distribution and into the recent results on asteroseismology of pre-white dwarfs.

Having all the basic stellar parameters it is easy to calculate the spectroscopic distances, following, for example, the method described in Méndez et al. (1992), which uses the stellar mass,  $\log g$ , monochromatic model atmosphere flux at visual wavelength, and dereddened apparent visual magnitude.

Table 2 shows these quantities and the resulting distances. They are not too different from the earlier spectroscopic distances by Méndez et al. (1988b, 1992), except for the effect of the different stellar masses we are using now. NGC 2392 gets a smaller distance and He 2-131 a larger one because the new mass is smaller and larger, respectively, than before.

**Table 2.** Computed spectroscopic distances of our sample stars and the quantities used to derive them. (See text.)

Object	Mass ( $M_{\odot}$ )	$\log g$ (cgs)	$F_{\star}$	$V$	$c$	distance (kpc)	$-\log F(\text{H}\beta)$	$M_{\beta}$
NGC 2392	0.41	3.70	7.48	10.53	0.16	1.67	10.29	0.5
NGC 3242	0.53	5.15	14.69	12.10	0.09	1.10	9.80	0.3
IC 4637	0.87	4.57	10.64	12.47	1.10	1.01	11.24	1.6
IC 4593	1.12	3.80	7.69	11.27	0.12	3.63	10.55	-0.5
He 2-108	1.33	3.70	7.49	12.82	0.40	6.76	11.41	-0.4
IC 418	1.33	3.70	7.49	10.00	0.32	2.00	9.62	-2.0
Tc 1	1.37	3.62	6.38	11.38	0.36	3.73	10.66	-0.8
He 2-131	1.39	3.10	6.26	10.50	0.14	5.62	10.16	-2.4
NGC 6826	1.40	3.90	8.61	10.69	0.04	3.18	9.97	-1.4

**Fig. 6.** The wind-momentum–luminosity relation for CSPNs (lower left) based on our values determined from the UV spectra (filled squares). The open squares are the values from Kudritzki et al. (1997) scaled to our determined radii, thus eliminating the need of an a-priori assumption for the radii, as was done by Kudritzki et al. (see text). Compared to Figure 1 the result is striking: now there is good agreement between the optical and UV mass loss rate determinations.

Now we want to discuss systematically how these spectroscopic distances compare with individual PN distances derived from other methods. We disregard all the statistical distances published by many authors because they are too uncertain for a case-by-case discussion. We consider in turn trigonometric parallaxes, distances derived from visual companions to the central stars, cluster distances, extinction distances, and expansion distances.

### 9.1. Trigonometric parallaxes

There is no overlap with the sample we are analyzing here. However, it is possible to compare trigonometric versus other spectroscopic parallaxes. Some ground-based trigonometric parallaxes are listed by Harris et al. (1997). We consider only those objects with reliable parallaxes larger than 2 milli-arc-seconds, i.e., with distances below 500 pc: NGC 6853,

NGC 7293, S 216. Their distances compare very well with the spectroscopic distances of Napiwotzki (1999).

The Hipparcos parallaxes again do not overlap with our sample, but again it is possible to compare with other spectroscopic parallaxes. Here there is some disagreement, especially in the case of PHL 932 and (marginally) A 36. The parallax for NGC 1360 is too uncertain, but Pottasch and Acker (1998) show convincingly that the Hipparcos distances of PHL 932 and A 36 require higher surface gravities than indicated by the spectroscopic analysis *if we assume a central star mass of  $0.6 M_{\odot}$* . One way to reduce the discrepancy is to reduce the mass of the central star; so in fact we could argue that Hipparcos has confirmed the conclusion that the central star of PHL 932 must have a very low mass, below  $0.3 M_{\odot}$ , and cannot be a post-AGB star (Méndez et al. 1988a). Napiwotzki (1999) has repeated the spectroscopic analysis of PHL 932, using different models and spectrograms, and obtains atmospheric parameters marginally consistent with those of Méndez et al. (1988a). His surface gravity is somewhat higher, but not as high as required by the Hipparcos parallax, unless we reduce the central star mass to the rather implausible value of  $0.1 M_{\odot}$ . Therefore in the case of PHL 932 some degree of contradiction remains. Would somebody please remeasure this parallax? Nowadays it can probably be done from the ground with adequate CCD techniques.

### 9.2. Distances derived from visual companions to the CSPNs

Again no overlap; but Ciardullo et al. (1999) assign a distance of 2.4 kpc to NGC 1535, in good agreement with the spectroscopic distance of 2.0 kpc in Méndez et al. (1992).

### 9.3. Cluster distances

Again no overlap. The only object we can mention here is the central star of the PN in the globular cluster M 15, where the spectroscopic distance is in excellent agreement with the cluster distance, see McCarthy et al. (1997).

#### 9.4. Extinction distances

Here finally we find some objects in common with our sample. Martin (1994) concludes that the extinction distance of He 2-131 (about 700 pc), although substantially smaller, does not necessarily invalidate our distance, in view of the high Galactic latitude of this PN. The same point was made earlier by Maciel (1985): given its high latitude, this object at a distance of 700 pc would be some 180 pc below the Galactic plane, which is not very different from the halfthickness of the Galactic absorbing layer. As a consequence, the extinction distance should be taken as a lower limit to the true distance. The same can be argued about Tc 1, with an extinction distance of 600 pc, although Martin considers this case more of a contradiction with the spectroscopic distance. For another of our objects (He 2-108) again there is no conflict.

Martin's best case of a contradiction is IC 2448, with an extinction distance of 840 pc and a spectroscopic distance of about 3 kpc. Unfortunately IC 2448 is not in the sample we are studying here; we do not know if a revised spectral analysis would reduce its spectroscopic distance somewhat. In any case, we think that one isolated discrepant case does not have too much weight, given the existence of many other cases showing agreement, because the isolated discrepancy can always be attributed to accidental fine structure in the interstellar dust distribution.

#### 9.5. Expansion distances

Again no overlap with our sample, but since we mentioned IC 2448 in the previous subsection, we should add that there is a recent expansion distance estimate for this PN by Palen et al. (2002). Their result is 1.4 kpc, apparently in better agreement with the extinction distance. Here we would like to sound a word of caution: a point which was made already some time ago by Steffen et al. (1997) and again by Schönberner (2001). The outer rim of a PN is defined by a shock front, the temporal displacement of which is not given by a material velocity and is not easily derivable from the Doppler splitting of the strongest PN emission lines. Hydrodynamic modelling indicates that frequently the Doppler splitting is smaller than the linear velocity of expansion in the plane of the sky. The assumption that both are equal can easily lead to systematically too small expansion distances, perhaps by a factor as large as 2. For that reason we think that some more work is needed on the interpretation of the angular expansion of PNs.

#### 9.6. Summary on distances

The amount of information is too small to extract any solid conclusion. The independent evidence would seem to provide support to several spectroscopic distances, but there are a few discrepant cases that need to be resolved.

Since we are primarily interested in testing the validity of the theory of post-AGB evolution, a few more comments are relevant. An interesting consequence of the extinction distances is that they produce several central stars with extremely low luminosities, which cannot be post-AGB stars (see Martin 1994).

Therefore we may still have a severe problem with the classical interpretation of several *other* CSPNs as post-AGB stars; similar to what we found for NGC 2392.

In this situation we need more and better independent distance determinations, good enough to convince everybody. For the moment, we find no compelling reason to reject the spectroscopic distances, although we understand that some of them are taken with skepticism. But we would expect the spectroscopic distances, if based on an inadequate physical theory, to fail all together in a very systematic way; not just a few of them wrong and all the others OK. And so we still expect that the few conflicting cases may be resolved in favor of the spectroscopic distances when more evidence is added.

#### 9.7. The constraints from the PN luminosity function

There is another verification we can undertake, based on the behavior of extragalactic PNs. They show a very characteristic luminosity function (PNLF), with a well-defined limiting brightness, which has been successfully used for extragalactic distance determinations (see, e.g., Jacoby and Ciardullo 1993, Jacoby 1997). We can try to verify if our spectroscopic distances produce any overluminous PN; that would be a nice argument supporting a smaller spectroscopic distance in that case.

Now one complication is that for extragalactic work the PNLF is built using the normally very bright nebular emission [O III]  $\lambda$ 5007. Very low-excitation PNs do not contribute to the bright end of the  $\lambda$ 5007 PNLF. But it turns out that some of our central stars belong to low-excitation PNs, implying that the flux in  $\lambda$ 5007 does not provide any useful limit. For that reason we have decided to do the test using a recombination line, namely H $\beta$ . The problem is now that we do not have too much observational information about the limiting H $\beta$  flux in other galaxies: the only well-observed case is the LMC. But we can try to supplement the observational LMC limit by a limit obtained from numerical simulations of the PNLF: see Méndez and Soffner (1997). Their Figure 6 shows the observed H $\beta$  LMC PNLF, compared with a simulated PNLF. Allowing for a somewhat larger sample size in our Galaxy (see the effect of increasing the sample size in Figure 10 of Méndez and Soffner), we can estimate that the brightest PNs in our Galaxy should have an absolute H $\beta$  magnitude of about  $-2.3$  (the relation between observed H $\beta$  flux and H $\beta$  apparent magnitude is traditionally defined as  $m_\beta = -2.5 \log F_\beta - 13.74$ ).

The resulting absolute H $\beta$  magnitudes we derive using our spectroscopic distances are listed in Table 2. There is only one case at the limit: He 2-131, with  $M_\beta = -2.4$ . All the other distances produce weaker absolute H $\beta$  magnitudes. Again we find no strong reason to reject our spectroscopic distances, although He 2-131 is admittedly at the very limit of acceptability.

#### 10. Masses of white dwarfs and pre-white dwarfs

Probably the most severe conflict we have is the large number of very massive CSPNs, in view of the known mass distribution of white dwarfs, with a well-defined maximum at about  $0.6 M_\odot$ . Although this could be used to argue against

the credibility of our analysis, we would like to point to the existence of some recent results involving very massive pre-white dwarfs and white dwarfs. Most interesting is a report by Kawaler (2001) who finds a wide range of pulsation periods among H-deficient CSPNs, which he tentatively interprets as due to a correspondingly large range of masses, from 0.52 to  $1.2 M_{\odot}$ . This looks surprisingly similar to our result, based on a completely different observational technique applied to a completely different sample of central stars (our stars have H-rich atmospheres).

Another study worth mentioning is by Napiwotzki et al. (1999). They have determined masses for a sample of 46 hot DA white dwarfs selected from the Extreme UV Explorer (EUVE) and ROSAT Wide Field Camera bright source lists. They find a peak mass of  $0.59 M_{\odot}$ , in agreement with many other studies, but find a non-negligible fraction of white dwarfs with masses in excess of  $1 M_{\odot}$ .

Yet another study by Silvestri et al. (2001), dealing with a sample of 41 white dwarfs in wide binary systems, finds a bimodal mass distribution with a second mass peak at  $1.1 M_{\odot}$ . They interpret this second peak, suspiciously close to twice the mass of the first peak, as the result of binary mergers.

Therefore, our mass distribution, with its probable dependence on very strong selection effects, is perhaps not as irreconcilable with the rest of the evidence as we could have thought initially.

The conflict with the post-AGB evolutionary speeds is not too important if we decide to accept a drastic departure from the relation between luminosity and mass. In this case new stellar structure and evolutionary calculations would be needed.

## 11. Conclusions and perspectives

We have applied our new model atmospheres, involving a much improved treatment of blocking and blanketing by all metal lines in the entire sub- and supersonically expanding atmosphere, to the analysis of a sample of 8 PN central stars. We have shown how the new models can produce an essentially perfect fit to a multitude of spectral features in the UV spectra of the CSPNs. The fits lead us to determine a set of stellar parameters including separate determinations of luminosity and mass, allowing for the first time a full test of the post-AGB evolutionary calculations. Surprisingly, we find drastic departures from the theoretical post-AGB mass–luminosity relation.

The luminosities we derive for the stars of our sample lie in the expected range, but we find a much larger spread in the masses, from 0.4 to  $1.4 M_{\odot}$ . The resulting relation between CSPN mass and luminosity deviates severely from that given by the theory of post-AGB evolution.

For five out of the nine CSPNs of our sample we obtain masses near, *but not above*, the critical Chandrasekhar mass limit for white dwarfs. Despite our sample most probably being influenced by selection effects, this result nevertheless invites speculation about the role of a group of CSPNs as precursors to the white dwarfs believed to end up as Type Ia supernovae.

We cannot at the moment offer a clear-cut explanation to the discrepancy between radiation-driven wind theory confirmed by UV-spectroscopy on the one hand and the theory

of post-AGB stellar evolution on the other (in particular the fact that from the former we derive masses both larger and smaller than those predicted by the latter); however, we point out a number of other independent observational investigations (see section 9) that have also found a similarly large spread (up to  $1.2 M_{\odot}$ ) in the CSPN/white-dwarf masses which cannot be explained by the classical post-AGB evolutionary theory. Nevertheless, if we believe both, the current evolutionary theory and the luminosities and masses we have determined from the atmospheric models, then most of the CSPNs of our sample have not followed a classical post-AGB evolution.

*Acknowledgements.* This work was supported by the Sonderforschungsbereich 375 of the Deutsche Forschungsgemeinschaft and by the DLR under grant 50 OR 9909 2.

## References

- Blöcker T., 1995, *A&A* 299, 755  
 Ciardullo R., Bond H. E., Sipior M. S., et al., 1999, *AJ* 118, 488  
 Harris H. C., Dahn C. C., Monet D. G., & Pier J. R., 1997, in proc. IAU Symp. 180, *Planetary Nebulae*, eds. H. J. Habing & H. J. G. L. M. Lamers, p. 40  
 Haser S. M., 1995, PhD-Thesis  
 Hoffmann T. L. & Pauldrach A. W. A., 2001, in proc. IAU Symp. 209, *Planetary Nebulae*, in press  
 Jacoby G., 1997, in proc. IAU Symp. 180, *Planetary Nebulae*, eds. H. J. Habing & H. J. G. L. M. Lamers, p. 448  
 Jacoby G. & Ciardullo R., 1993, in proc. IAU Symp. 155, *Planetary Nebulae*, eds. R. Weinberger & A. Acker, p. 503  
 Kawaler S. D., 2001, *ASP Conf. Series* 226, p. 287  
 Kudritzki R.-P., Méndez R. H., Puls J., & McCarthy J. K., 1997, in proc. IAU Symp. 180, *Planetary Nebulae*, eds. H. J. Habing & H. J. G. L. M. Lamers, p. 64  
 Maciel W., 1985, *Rev. Mex. Astr. Astrof.* 10, 199  
 Martin W., 1994, *A&A* 281, 526  
 McCarthy J. K., Méndez R. H., Becker S., Butler K., & Kudritzki R.-P., 1997, in proc. IAU Symp. 180, *Planetary Nebulae*, eds. H. J. Habing & H. J. G. L. M. Lamers, p. 122  
 Méndez R. H., Groth H. G., Husfeld D., Kudritzki R.-P., & Herrero A., 1988a, *A&A* 197, L25  
 Méndez R. H., Kudritzki R.-P., Herrero A., Husfeld D., & Groth H. G., 1988b, *A&A* 190, 113  
 Méndez R. H., Kudritzki R.-P., & Herrero A., 1992, *A&A* 260, 329  
 Méndez R. H. & Soffner T., 1997, *A&A* 321, 898  
 Napiwotzki R., 1999, *A&A* 350, 101  
 Napiwotzki R., Green P. J., & Saffer R. A., 1999, *ApJ* 517, 399  
 Palen S., Balick B., Hajian A. R., et al., 2002, *AJ* 123, 2666  
 Pauldrach A. W. A., 1987, *A&A* 183, 295  
 Pauldrach A. W. A., Puls J., Kudritzki R.-P., et al., 1988, *A&A* 207, 123  
 Pauldrach A. W. A., Hoffmann T. L., & Lennon M., 2001, *A&A* 375, 161  
 Pauldrach A. W. A., Hoffmann T. L., Méndez R. H., 2001a, in proc. IAU Symp. 209, *Planetary Nebulae*, in press  
 Pauldrach A. W. A., 2003, *Rev. Mod. Astron.* Vol. 16, 141–177  
 Pauldrach A. W. A. & Hoffmann T. L., 2003, *A&A*, in prep.  
 Pottasch S. R. & Acker A., 1998, *A&A* 329, L5  
 Puls J., Kudritzki R.-P., Herrero A., et al., 1996, *A&A* 305, 171  
 Schönberner D., 2001, in proc. IAU Symp. 209, *Planetary Nebulae*, in press  
 Scuderi S., Panagia N., Stanghellini C., et al., 1998, *A&A* 332, 251

- Silvestri N. M., Oswalt T. D., Wood M. A., et al., 2001, ASP Conf. Series 226, p. 246
- Steffen M., Schönberner D., Kifonidis K., & Stahlberg J., 1997, in proc. IAU Symp. 180, Planetary Nebulae, eds. H. J. Habing & H. J. G. L. M. Lamers, p. 368
- Tinkler C. M. & Lamers H. J. G. L. M., 2002, A&A 384, 987